MSC 76-04 **DOI: 10.14529/mmp210306**

APPLICATION OF THE FINITE VOLUME METHOD FOR CALCULATING RADIATION HEAT TRANSFER IN APPLIED PROBLEMS

***K.Yu. Litvintsev*[1], *A.V. Sentyabov*[1]**
[1]Krasnoyarsk Division, S.S. Kutateladze Institute of Thermophysics, SB RAS, Krasnoyarsk, Russian Federation
E-mail: sttupick@yandex.ru, sentyabov_a_v@mail.ru

A number of numerical models of radiation heat transfer, based on P_1 approximation and finite volume method, were implemented in the in-house CFD code "SigmaFlow" developed by the Krasnoyarsk group of the Institute of Thermophysics of Russian Academy of Science. The implemented finite volume method allows parallel calculations based on domain decomposition of an unstructured mesh and uses sub-mapped spatially inhomogeneous angular grids. Both conventional in CFD methods for solving linear systems such as BiCGStab, DILU, CG and a marching scheme were considered. A number of applied problems with radiation heat transfer were solved by means of CFD code "SigmaFlow". They include such problems as the numerical simulation of a gas furnace chamber, a burner and a vacuum electrical furnace.

Keywords: radiation heat transfer; finite volume method; numerical simulation.

Introduction

When using numerical simulation to solve a wide class of applied problems, it is very important to adapt the mathematical models of the processes in order to reduce the computational cost keeping an acceptable accuracy. This is especially relevant for simulation of radiation transfer problems, which can demand considerable computational resources due to anisotropy in radiation and the dependence of the optical properties of the medium on the radiation frequency. When developing the SigmaFlow software package [1] for solving applied problems of computational fluid dynamics and heat transfer, the Krasnoyarsk Division of S.S. Kutateladze Institute of Thermophysics developed mathematical models of radiation transfer based on the use of the P_1 approximation [2, 3] and the finite volume method [4]. In addition, the discrete-ordinate method (DOM) based on S_n-quadratures [5] was implemented for comparison [6]. While the P_1 approximation was used for quite a long time, the finite volume method (FVM) for solving the radiation transfer equation appeared and began to actively develop only in the 90s of the last century, but now is widely used [4, 7–11]. It is especially worth to note the use of the FVM in such freeware products as OpenFOAM and FDS (NIST), designed for numerical simulation of the processes associated with fluid dynamics and heat and mass transfer. The FVM is the optimal method for simulating the radiation heat transfer. Therefore, the FVM has no restrictions on the optical properties of the medium (inhomogeneity, anisotropy, scattering) in contrast to the P_n approximations (especially P_1), the discrete transfer method. In addition, this method does not make special requirements for the computational domain in contrast to the flux methods. FVM gives less accuracy than ray-based methods such as Monte Carlo method, but it requires less computational resources. At the same time,

FVM requires a bit more computational resources [12] than discrete-ordinate method but it describes radiation scattering more precisely. The FVM is conservative and provides flexible angular discretization. As well, an advantage of the FVM is its relatively simple and clear derivation in the case of the radiative transfer equation [7, 13]. In addition, there exists a number of approaches based on the simultaneous use of several methods for solving radiative transfer equation, for example [14, 15]. This paper discusses the combined use of the FVM and the P_1 approximations as well.

1. Mathematical Model

1.1. Radiative Transfer Equation

The radiative transfer equation (RTE) describes the energy balance at a given frequency of radiation entering along the $\vec{s}$ direction into a small volume of the absorbing, emitting and scattering medium:

$$\frac{dI_\nu(\vec{r},\vec{s})}{ds} = -\beta_\nu(\vec{r})\, I_\nu(\vec{r},\vec{s}) + \kappa_\nu(\vec{r})\, I_{b\nu}(\vec{r}) + \frac{\sigma_\nu(\vec{r})}{4\pi}\int\limits_{4\pi} I_\nu(\vec{r},\vec{s}')\,\Phi(\vec{s}',\vec{s})\,d\Omega', \qquad (1)$$

where I_ν is the radiant intensity; $I_{b\nu}$ is the radiant intensity of black body; β_ν is the extinction coefficient ($\beta_\nu = k_\nu + \sigma_\nu$); k_ν is the absorption coefficient; σ_ν is the scattering coefficient; Ω is the solid angle; $\vec{r}$ is the spatial position; $\vec{s}$ is the angular direction; Φ_ν is the scattering phase function. Further, in the equations, the subscript ν will not be used.

Gray gas models, WSGG (Weighted Sum of Gray Gases) models and spectral models based on HITRAN (HIgh-resolution TRANsmission) molecular absorption database [16] were used to define the absorption coefficient of the medium.

1.2. Finite Volume Method

FVM is based on the spatial and angular discretization of radiant intensity by means of splitting the computational domain into control volumes and control solid angles, respectively (Fig. 1). The RTE (1) is discretized by integration over both spatial control volume and angular control (solid) angle. Replacing the volume integral by the surface integral we obtain [4, 7]:

$$\int\limits_{\Delta\Omega^l}\int\limits_{\Delta A} I^l\left(\vec{s}^{\,l}\cdot\vec{n}\right)dAd\Omega = \int\limits_{\Delta\Omega^l}\int\limits_{\Delta V}\left(-\beta I^l + S^l\right)dVd\Omega, \qquad (2)$$

$$S^l = \kappa I_b + \tfrac{\sigma}{4\pi}\sum_{l'=1}^{L} I^{l'}\bar{\Phi}^{l'l}\Delta\Omega^{l'},$$

where $\Delta\Omega^l$ is a control solid angle; subscript nb means a face of the node P; $\bar{\Phi}^{l'l}$ is the averaged scattering phase function from the control angle l' into the control angle l, $\vec{n}$ is the normal, ΔA is the area of the control volume face.

As a result, the discrete form of equation (1) for arbitrary spatial grids in the l-th direction of radiation transfer can be written as follows:

$$\sum_{nb} I^l_{nb}A_{nb}D^l_{nb} = \left(-\beta I^l_p + S^l\right)\Delta V\Delta\Omega^l, \qquad (3)$$

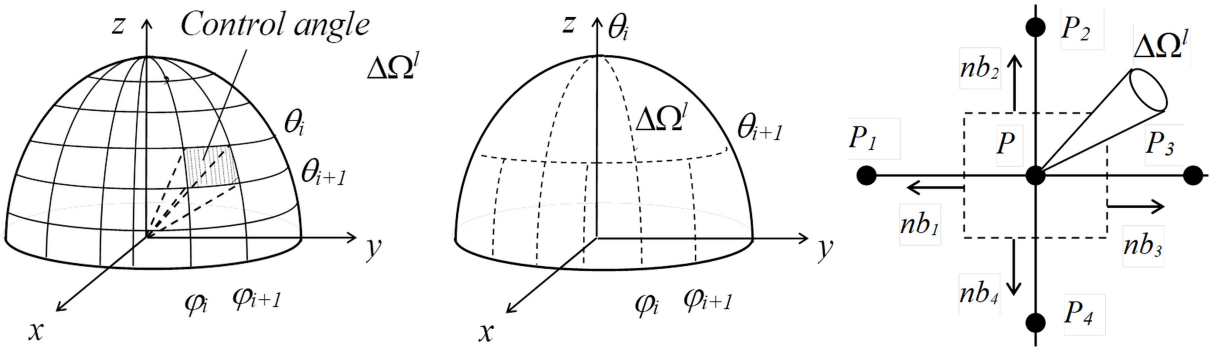

Fig. 1. Spatial and angular discretization of the radiative transfer equation: a) an uniform angular discretization; b) a nonuniform angular discretization; c) a control volume and an angular direction

$$D_{nb}^{l} = \int\limits_{\Delta\Omega^{l}} \left(\vec{s}^{\,l} \cdot \vec{n}_{nb}\right) d\Omega,$$

where the subscript nb is a number of the control volume face; the subscript P is a number of the control volume.

Using the upwind differencing scheme, a node value of the intensity approximates the value of intensity in the faces placed along the beam propagation. The discrete form of the equation obtained by the FVM and upwind scheme on arbitrary grids is written as follows:

$$a_P^l I_P^l = \sum_{nb} a_{nb}^l I_{nb}^l + b^l, \tag{4}$$

$$a_{nb}^l = \max\left(-A_{nb} D_{nb}^l, 0\right), \quad a_P^l = \sum_{nb} \max\left(A_{nb} D_{nb}^l, 0\right) + \beta_P \Delta V_P \Delta\Omega^l, \quad b^l = S_P^l \Delta V_P \Delta\Omega^l.$$

In equation (4), the incoming radiant intensity I_{nb} ($D_{nb} < 0$) is assumed to be known and the outcoming radiant intensity I_{nb} ($D_{nb} > 0$) is assumed equal to I_P.

To reduce the error made by the intersection of the faces of the control volumes with the control solid angles, the solid angle Ω^l is divided by the face into two solid angles Ω^{l+} and Ω^{l-} corresponding to the inflow and outflow radiative heat fluxes (Fig. 2). In this case, equation (4) is modified as follows:

$$a_{nb}^l = -A_{nb} D_{nb}^{l+}, \tag{5}$$

$$D_{nb}^{l\pm} = \int\limits_{\Delta\Omega^{l\pm}} \left(\vec{s}^{\,l} \cdot \vec{n}_{nb}\right) d\Omega, \quad a_P^l = \sum_{nb} A_{nb} D_{nb}^{l-} + \beta_P \Delta V_P \Delta\Omega^l.$$

The subscripts "+" and "–" correspond to the inflow and outflow radiative heat fluxes of control volume P.

It is advisable to use this modification with a coarse angular grid; otherwise, the effect of this error is minimal.

Periodic boundary conditions and boundary conditions for an opaque diffuse surface were implemented. The diffuse surface boundary condition is the most popular condition in

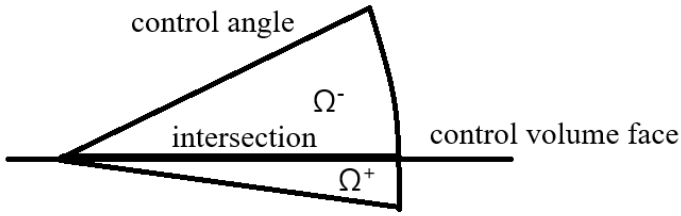

Fig. 2. An example of the intersection of a control angle with a control volume face

applied problems, both due to the predominance of surfaces with the blackness degree close to unity, and due to the lack of the radiant reflection and emission intensity distribution.

To solve linear algebraic equations (4), (5), such standard methods as both BiCGSTAB, DILU, CG etc. and a space-marching method can be used [7]. The advantage of the former methods is that they were already implemented to solve fluid dynamics and they use the same general data structure. The space-marching algorithm is a sequential calculation of the radiant intensity in the control volumes in the chosen direction.

2. Examples of Problems That Use FVM with P_1 Approximation

For many applied problems of computational fluid dynamics with radiation heat transfer, the P_1 approximation is still used to solve the RTE. This is justified when the problem is characterized by weak anisotropy of the radiation field. The papers [17, 18] show that, in the case of an isotropic or weakly anisotropic medium, the P_1 approximation is accurate enough and the results of the calculation of the radiation field obtained for optically thin media ($\tau \ll 1$) are often more accurate than those obtained for optically thick. However, when solving problems with complex geometry and inhomogeneous optical properties of the medium, the P_1 approximation is mostly used for optically thick media ($\tau > 1$) [19] or when the radiation flux distribution at the boundary is not interested. In the same paper [17] it was shown that the error in calculating the radiation flux to the wall becomes higher in optically thin media as the radiation field anisotropy increases due to inhomogeneous boundary conditions or optical properties of the medium.

When it is necessary to take into account the dependence of the optical properties of the medium on the radiation frequency, the use of the P_1 approximation leads to significant errors for some spectral bands or "gray" gases. In this case, it is necessary to use more accurate, but also more expensive, methods for solving the RTE, particularly FVM. However, the advantages of the P_1 approximation can be applied in this case as well. In fact, for numerical simulation of radiation transfer using WSGG or band models, the RTE is solved for a number of the media with its own "grey" gas properties. This makes it possible to use the combined approach when, e.g., the P_1 approximation is used for calculating optically thick media, and FVM is used for the other media [20]. Thus, the total value of the radiation flux can be described by the following expression:

$$E(\vec{r}) = \sum_{i}^{N_i} E_i^{\mathrm{FVM}}(\vec{r}) + \sum_{j}^{N_j} E_j^{P_1}(\vec{r}), \tag{6}$$

$$E(\vec{r}) = \int_{4\pi} I(\vec{r}, \vec{s})\, d\Omega, \tag{7}$$

where N_i и N_j are "gray" gases calculated by FVM and P_1 approximation, respectively, E is the incident radiation flux (W/m^2).

In this case, the radiation source term in the energy conservation equation is as follows:

$$\nabla q = \sum_{i}^{N_i} k_i \left(E_i^b \left(\vec{r} \right) - E_i^{\mathrm{FVM}} \left(\vec{r} \right) \right) + \sum_{i}^{N_j} k_j \left(E_j^b \left(\vec{r} \right) - E_j^{P_1} \left(\vec{r} \right) \right), \tag{8}$$

where E^b is the outcoming radiation flux of the black body for the i-th or j-th gray gas.

The described approach shows significant advantages when using WSGG models in which it is easy to define an optically thick medium for one of the "gray" gases. For example, for the WSGG model proposed in [21], the values of the absorption coefficients of gray gases are as follows: 131,9 m^{-1} atm^{-1} for the first, 6,516 m^{-1} atm^{-1} for the second and 0,4201m^{-1} atm^{-1} for the third, 0 m^{-1} atm^{-1} for the fourth. In the majority of cases, the first "gray" gas can be calculated by the P_1 approximation. For the second and third gases, it is necessary to estimate the distribution of concentrations of reference gases (CO_2 and H_2O) and the characteristic length of the problem more accurately. It should be noted that the approach was also considered in the paper [17] for the SLW model (spectral-line-based WSGG) where the P_1 approximation was also used for gray gases with the highest absorption coefficient.

2.1. Closed Cylinder Filled with Gas Mixture

Consider the use of the combined approach on the example of a test problem presented in the paper [22], where DOM with 96 directions in conjunction with the WSGG absorption coefficient model was used to calculate the radiation transfer. The problem domain is a closed cylinder filled with a gas mixture with a uniform temperature (Fig. 3a). The volume fraction of H_2O, CO_2 and N_2 was 20%, 10% and 70%, respectively.

The solution of radiation heat transfer was based on the FVM with 96 discrete directions to calculate the absorption coefficient. The WSGG model [21] was used. Comparison of the radiation flux on the sidewall of the cylinder was carried out. The solution obtained using the P_1 approximation for the first gray gas of the WSGG model and the FVM for the other gases agrees with the solution obtained using only the FVM and the results presented in [22] (Fig. 3b). When the first two "grey" gases are calculated on the basis of the P_1 approximation, some deviations are observed near the bottom side of the cylinder (Fig. 3b), that is, for the second "grey" gas the medium is not sufficiently optically thick.

Thus, for this problem, the time consumption of radiation transfer calculation was reduced by about 25% without losing the accuracy of the solution.

2.2. Burning Anode Gases of Aluminium Production

The combined approach was used in modelling the operation of some equipment. The first problem was a burner device (Fig. 4) intended for burning the anode gas of an electrolysis production. Anode gases released in the process of electrolysis production of aluminium consist mainly of CO (up to 55%), CO_2 (up to 70%) and N_2. In this problem, we consider a variant of the composition of the anode gas with volume concentrations 30% of CO and 35% of CO_2. The anode combustible gases enter the burner device from below

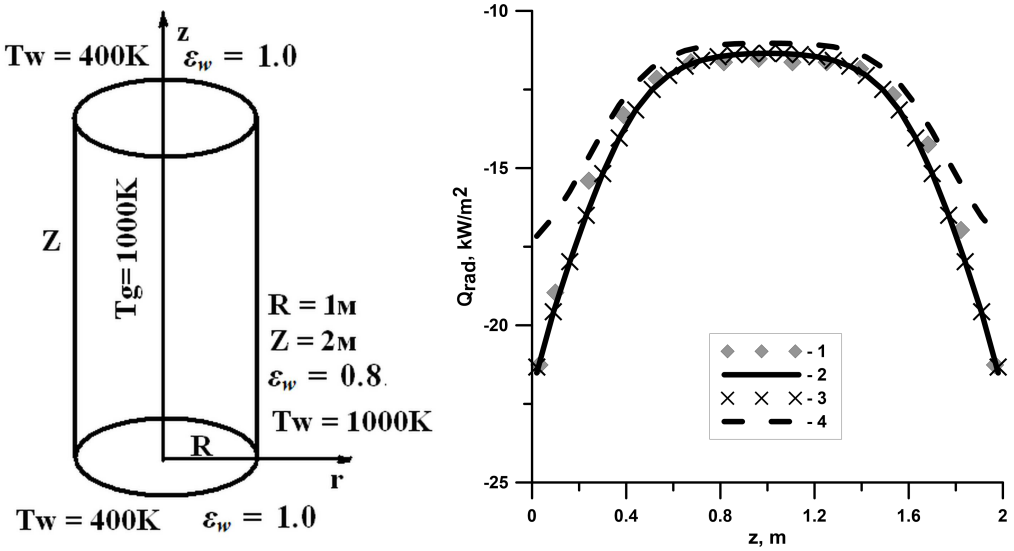

a) b)

Fig. 3. Closed cylinder filled with a gas mixture: a) the scheme, b) the radiation flux on the sidewall of the cylinder: 1 – [22]; 2 – FVM; 3 – FVM and P_1 approximation for single "grey" gas; 4 – FVM and P_1 approximation for two "grey" gases

with a temperature 800 ^{o}C. Then they are diluted with air entering from the environment through the side slots.

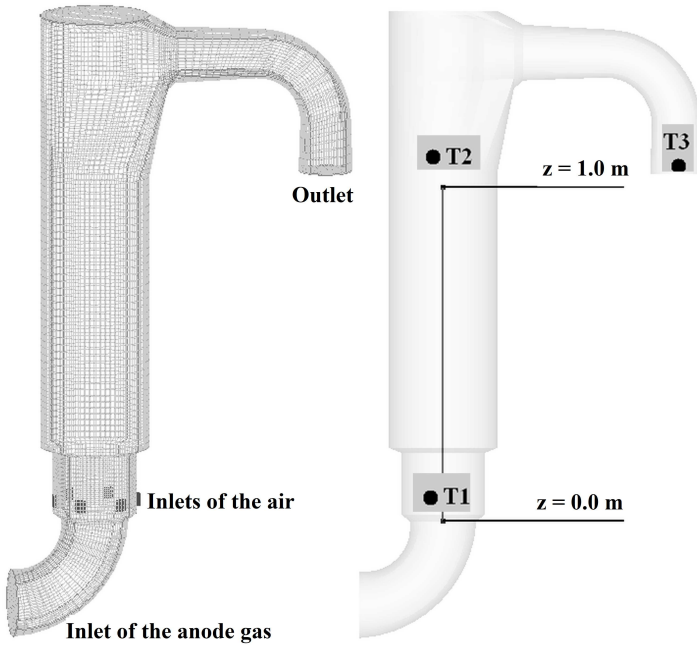

a) b)

Fig. 4. The burner device: a) grid; b) plots line and monitoring points

The need to use spectral models of the absorption coefficient is associated with a significant underestimating of the temperature when using the approximation of the "grey" gas (Fig. 5b, 6a). Using the WSGG model for the absorption coefficient led to an increase in the calculation time, almost in proportion to the number of "grey" gases in the model.

The results of combined FVM and P_1 approximation for single "grey" gas approach differ from the results of only FVM in the mixing zone of cold air with anode gas (Fig. 5a, 5b, 6b). In this area, in comparison with the calculation by FVM, the average temperature is reduced by 80 ^{o}C. This is due to the fact that, in this zone, the high-temperature radiating region has a small characteristic length, and thus, despite the high absorption coefficient for the first gray gas in the WSGG model, the medium is not sufficiently optically thick for the P_1 approximation. However, since this area of combustion is rather small, the differences in temperature above the mixing zone are not so large, no more than 20 ^{o}C (Fig. 5, 6a). Thus, the combined use of the FVM and P_1 approximations (even with single "grey" gas) in this problem can decrease the accuracy of the numerical simulation results of combustion in the mixing region.

a) b) c)

Fig. 5. Temperature field in a vertical cross-section, ^{o}C: FVM, 32 control angles, WSGG; b) FVM, 32 control angles, 15-bands model; c) FVM with P_1, 32 control angles, WSGG

In addition, a 15-band model based on the HITRAN database was compared with the WSGG model of the absorption coefficient for the burner device. The temperature fields calculated by the 15-band and WSGG models appear close to each other. The temperature difference was about 100 ^{o}C (Fig. 5, 6a). The main differences were observed near the entrance to the burner where the radiation heat loss calculated with a 15-band model exceeded the loss calculated by the WSGG model. This is due to the fact that, in the WSGG model, the absorption coefficient is calculated from CO_2 and H_2O volume fraction, thus, a large amount of CO in the anode gas was not taken into account. This fact leads to an underestimation of the absorption coefficient and, in the end, to the slightly higher average temperature in the burner compared to the band model.

Table presents the results of the comparison of the measured data with the data calculated by means of different models of the absorption coefficient. In general, it can be seen that, in the calculation of the burner device, the use of the no-"gray" absorption coefficient models makes it possible to obtain a temperature level corresponding to the measurement data. The discrepancies in temperature ranges in the experiment and

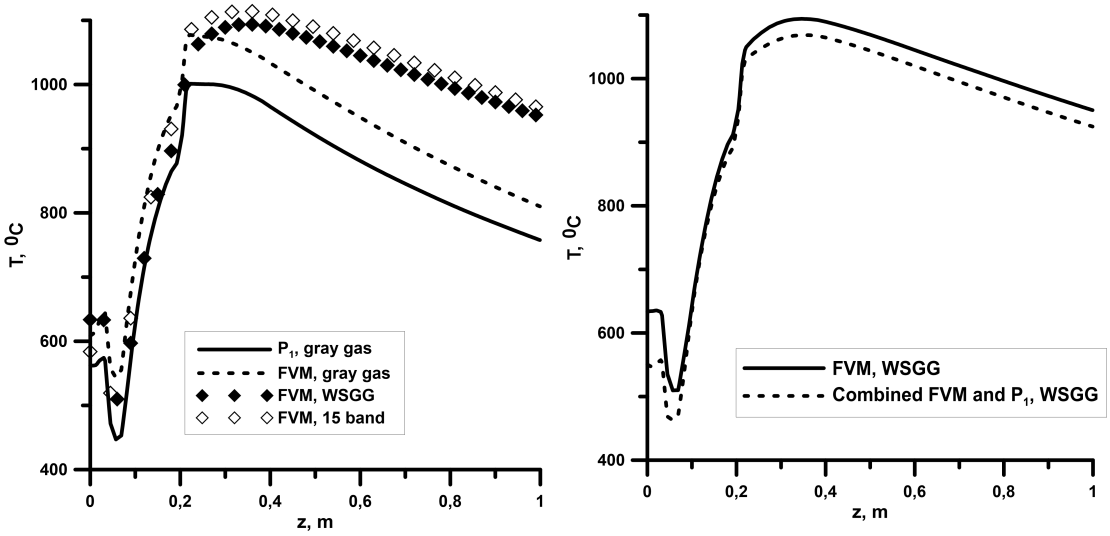

a) b)

Fig. 6. Distribution along the z-axis of the temperature averaged in the burner cross-sections: a) comparison of the results of different radiation and absorption coefficient models, b) comparison of the results of the FVM with and without P_1 approximation from the first "grey" gas in WSGG model

Table

Comparison of the calculated temperatures, ^{o}C, in horizontal cross-sections with the measured at the monitoring points (Fig. 5b)

monitoring points	WSGG model	15-band model	"grey" gas approximation	measured data
T1	900–950	840–880	900–950	870–945
T2	800–900	790–890	640–700	780–990
T3	670–750	660–740	500–550	620–845

calculations are related to the fact that the calculation does not cover all the operating modes of the burner. For example, with an increase in the total flow rate by 15%, the temperature increases by an average of 20–30 ^{o}C. The greatest discrepancy with the measurement data is observed at the point 1, which is associated with the peculiarity of measurements due to the strong irregularity of the temperature and velocity fields over the cross-section of the burner. Since a high temperature is observed in the center of the burner, which is primarily monitored during a series of point measurements, the resulting measured average temperature appears higher than the true average temperature. In the case of using the "grey" gas approximation, the temperature in the burner device is significantly lower compared with the measurement data (Table).

2.3. Gas Furnace

This problem considers a gas furnace of 250 MW power. Methane was used as a gas fuel, during the combustion of which H_2O and CO_2 are released. The computational mesh consists of 160 000 control volumes (Fig. 7a). When using the grey-gas approximation, the

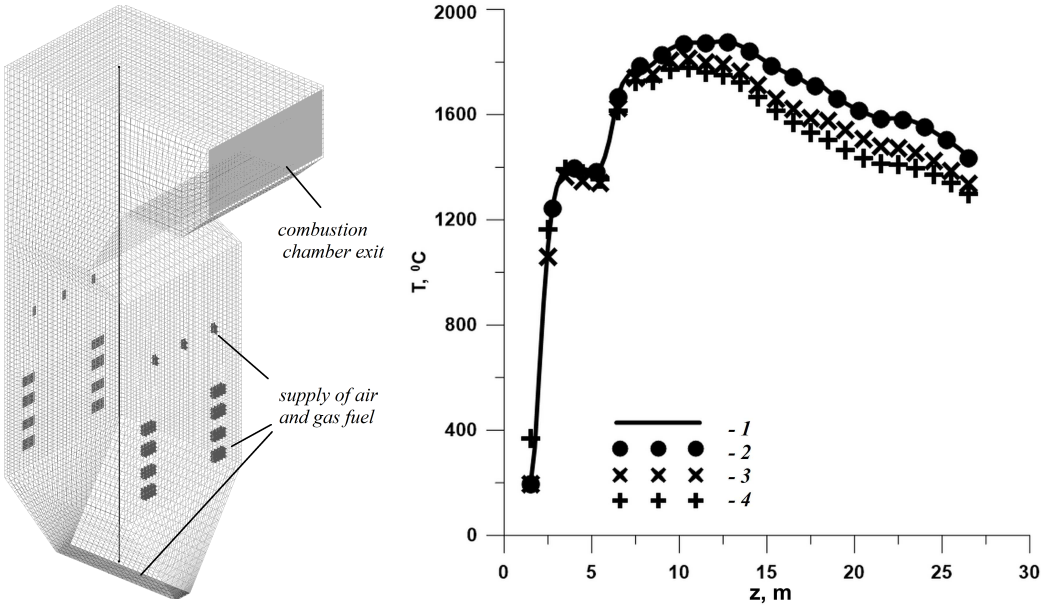

a) b)

Fig. 7. Gas furnace: a) scheme of the gas furnace and computational mesh; b) distribution of the averaged over a cross-section temperature along z-axis, ^{o}C: 1 – FVM, 2 – FVM with P_1 approximation for one "gray" gas, 3 – FVM, "gray" gas approximation, 4 – P_1 approximation for the "gray" gas

radiation transfer was calculated by two methods: the FVM and the P_1 approximation. In the case of the P_1 approximation, the temperature in the core of combustion and in the area above the air supply points is slightly higher than the results of FVM, but the temperature difference decreases closer to the exit from the combustion chamber (Fig. 7b). The only significant difference is observed in the lower part of the furnace, into which air enters (Fig. 8c). As a result, the medium in that zone is optically transparent; accordingly, the P_1 approximation does not work correctly.

When using the WSGG model [21], the difference is not so strong compared to the previous example (Fig. 6), but, in this case, taking into account the selectivity of the medium leads to an increase in temperature in the combustion chamber and a change in the temperature distribution as compared to the "gray" gas approximation. The most noticeable difference in the gas temperature calculated by means of WSGG and "gray" gas models can be seen in the combustion core (Fig. 7b, 8a, 8b). The vertical distribution of the temperature averaged over the horizontal furnace cross-section shows that using the "grey" gas model leads to a decrease in the averaged temperature by 100 ^{o}C maximally for the FVM and 140 ^{o}C for the P_1 approximation compared to the WSGG model. The results of the analysis of the calculations show the need to take into account the selectivity of radiation to simulate the gas furnace.

The combined use of the FVM and P_1 approximation with the WSGG absorption coefficient model (for the first "grey" gas) gives a solution that is almost identical to the solution obtained by only the FVM (Fig. 7b). This result is associated with the presence of significant concentrations of radiating gases (a mixture of H_2O and CO_2 up to 30%), and with large scales of the combustion chamber (in contrast to the previous problem with a burner).

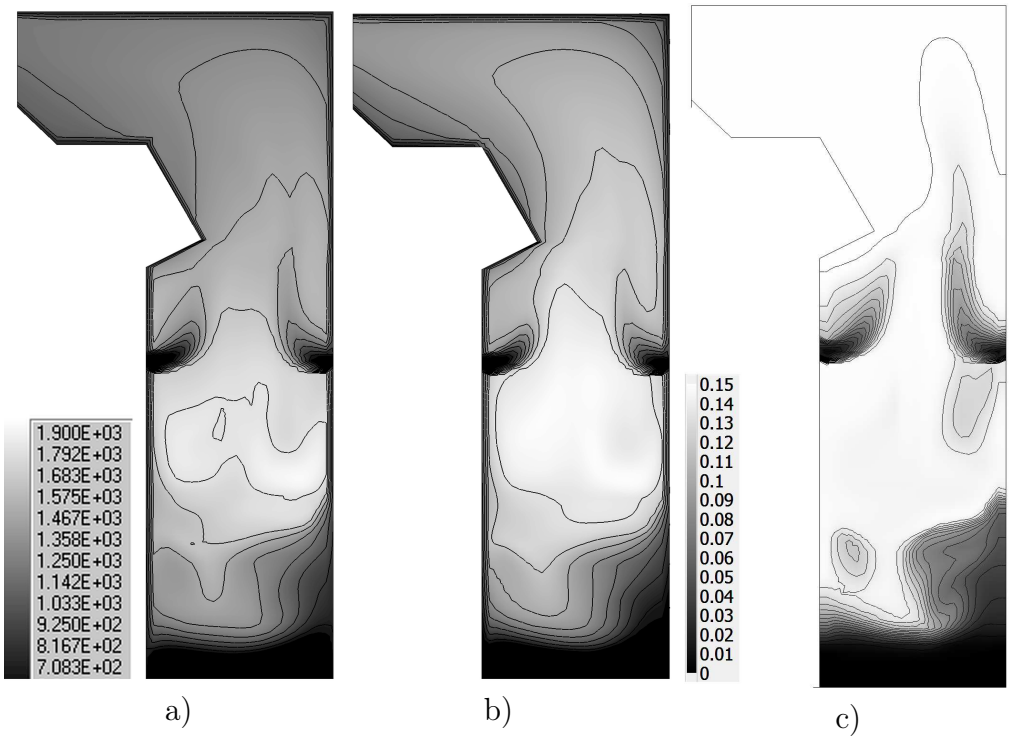

Fig. 8. Gas furnace: a) temperature for "grey" gas approximation with P_1 approximation, ^{o}C; b) temperature for WSGG model with the FVM, ^{o}C; c) CO_2 concentration, kg/kg

3. Marching Scheme for FVM with Unstructured Grids

Both created by the in-house mesh generator and imported from other programs unstructured grids are used for mathematical modelling of geometrically complex equipment in SigmaFlow. A FVM for the radiation transfer on unstructured grids was developed to solve such problems with complex geometry. In addition, parallel computing based on the spatial decomposition of the computational domain was implemented.

Features of the implementation of the FVM are presented on the example of solving the problem of modelling coupled heat transfer in a vacuum electric resistance furnace.

3.1. Optimization of Mathematical Model for Calculating Radiation Transfer for Vacuum Electric Furnace

A vacuum electric furnace is an object with a working space of 14,7 m^3 having electric resistance heating elements (in the form of a column), the lining and internal equipment made of carbon materials. Two retorts, external and internal, are placed inside the furnace. The main technological process takes place inside the smaller retort. The characteristic cycle time of the furnace is several days; the maximum heating temperature inside the working area is about 1800 ^{o}C. The pressure in the furnace is maintained at a few hundred Pa. The mechanism of the heat transfer by radiation in an electric furnace is dominant [23, 24]. The main problems in the simulation of heat transfer in this furnace are related to the duration of the technological process and the different scale of elements (from several millimeters to meters), which lead to long computing times (mesh consists of $5 \cdot 10^6$ cells).

During the numerical simulation of the electric furnace, most of the time is wasted on the radiation calculation, therefore, the optimization of the mathematical model of

radiation transfer based on the use of the FVM was carried out to reduce time costs.

First, the FTn modification of the FVM for the angular discretization was implemented to reduce the calculation time. This method allows a more uniform division of the angular space, compared to the standard approach based on the uniform discretization of spherical angles (Fig. 1a, b) [25–27]. The FTn modification of the FVM allows the use of smaller number of discrete solid angles compared to standard angular partitioning. In this problem, this allowed to reduce angular discretization from 32 discrete solid angles to 24 without a significant change in the calculated radiation field.

Further, the problem was used for comparison of methods for linear equations solving, which is implemented in SigmaFlow to solve problems of hydrodynamics and heat transfer. There were such methods as the incomplete LU-factorization method (DILU), the stabilized bi-conjugate gradient method (BiCGSTAB), the conjugate gradient method (CG) and a marching scheme implemented for unstructured grids [7, 28–30]. This comparison included multi-threaded calculations based on the spatial decomposition of the computational domain.

Construction of an unstructured grid using the in-house grid generator of "SigmaFlow" includes hexahedral (mostly) and four- and five-sided control volumes. With the correct construction of the grid, all the control volumes (cells) are convex, which makes it possible to find an effective traversal algorithm for a marching scheme. An effective traversal algorithm implies that, if the degree of blackness for all boundaries is equal to one and the absence of dispersion, the radiation field is calculated in a single pass. Test calculations showed that, in an optically thin medium, time of calculation for an effective traversal algorithm of the marching scheme is up to 11 times less than for standard methods implemented in SigmaFlow. In addition, it turned out that the BiCGSTAB method and other Krylov-type methods (CRES, CG) may not find the solution for zero right-hand side, i.e. when the medium is optically transparent. Therefore, for calculations of radiation transfer in an electric furnace, the marching scheme was compared with DILU.

A drawback of the marching scheme is that it becomes iterative and its efficiency decreases for geometrically complex objects, using the error reduction procedure associated with angular overlap, and for parallel multi-threaded calculations based on spatial decomposition. Numerical simulation of conjugate heat transfer in an electric furnace is an example of such a problem, which meets these conditions.

The calculations of the radiation field for the electric furnace showed that the marching scheme accelerates the calculation of the radiation field by about 5.5 times compared to DILU for a serial calculation. When using multi-threaded calculations, this ratio changes and can both decrease and increase. This is due to the presence of solid bodies, in which, when using the marching scheme, the calculation is not performed, and therefore the efficiency of the multi-threaded calculations strongly depends on the decomposition of the computational domain, i.e. how evenly the fluid region is distributed. This is clearly seen from the comparison of the calculations where the radiation field is calculated in the entire computational domain with those where the radiation field is calculated only in a part of the computational domain. If the computational domain is completely transparent to radiation, then the efficiency coefficient of multi-thread calculations is close to unity. However, in this problem with solids, its value is significantly lower than unity and varies considerably depending on the "quality" of the partition. For example, its value varies from 0,57 to 0,62 with decomposition into 2–6 parts.

Conclusions

The paper presents a brief description of the methods for solving the radiative transfer equation that were implemented in the in-house program package "SigmaFlow" and some examples of applied problems in which radiation heat transfer plays an important role. Each of the considered examples was a kind of optimization problem aimed at a balance between the required accuracy of the solution and computational costs. For the burner and gas furnace, the optimal absorption coefficient model and the numerical methods were defined. On the other hand, for the electric furnaces problem, the optimal methods for solving the linear equations and partitioning the angular space were determined. In addition, the example of the electric furnace shows the influence of the spatial decomposition of the computational domain in multi-threaded calculations on the parallelization efficiency of the conjugate heat transfer problems. The problems considered show that it is possible to reduce computational requirements without significantly reducing the accuracy of calculations by adapting numerical methods and mathematical models to specific applied problems.

The methods for calculating the radiation heat transfer implemented in the SigmaFlow program package showed their capabilities in solving applied problems. Analysis of the results shows that the presented approaches can be further developed to increase their effectiveness. This concerns such approaches as the combined use of the P_1 approximation and the FVM (when not only a number of different "grey" gases but also a spatial separation of the approaches are used), more complex partition of the angular space and more efficient spatial decomposition algorithms for conjugated problems.

Acknowledgement. *This work was carried out under state contract with IT SB RAS (0257-2021-0001).*

References/Литература

1. Dekterev A.A., Litvintsev K.Yu., Gavrilov A.A., Kharlamov E.B., Filimonov S.A. The Development of Free Engineering Software Package for Numerical Simulation of Hydrodynamics, Heat Transfer, and Chemical Reaction Processes. *Bulletin of the South Ural State University. Series: Mathematical Modelling, Programming and Computer Software*, 2017, vol. 10, no. 4, pp. 105–112. DOI: 10.14529/mmp170410
2. Jeans J.H. The Equations of Radiative Transfer of Energy. *Monthly Notices Royal Astrojwmical Society*, 1917, no. 78, pp. 28–36.
3. Eddington A.S. *The Internal Constitution of the Stars*, New York, Dover Publications, 1959.
4. Raithby G.D., Chui E.H. A Finite-Volume Method for Predicting a Radiant Heat Transfer Enclosures with Participating Media. *Journal of Heat Transfer*, 1990, no. 11, pp. 415–423.
5. Fiveland W.A. A Discrete Ordinates Method for Predicting Radiative Heat Transfer in Axisymmetric Enclosures. *ASME Paper*, 1982, no. 82-HT-20, 1982.
6. Litvintsev K.Yu, Dekterev A.A. Comparison of the Finite-Volume and Discrete-Ordinate Methods and Diffusion Approximation for the Radiative Heat Transfer. *Heat Transfer Research*, 2008, vol. 39, pp. 653–655.
7. Chai J.C., Patankar S.V. *Finite-Volume Method for Radiation Heat Transfer, in Advances in Numerical Heat Transfer*, New York, Taylor and Francis, 2000.

8. Wray A. Improved Finite-Volume Method for Radiative Hydrodynamics. *International Conference on Computational Fluid Dynamics*, 2012, article ID: 20120016552.
9. Lygidakis G.N., Nikolos I.K. Improving the Accuracy of a Finite-Volume Method for Computing Radiative Heat Transfer in Three-Dimensional Unstructured Meshes. *Proceedings of the 3rd South-East European Conference on Computational Mechanics*, Greece, 2013, pp. 599–620.
10. Trovalet L., Jeandel G., Coelho P.J., Asllanaj F. Modified Finite-Volume Method Based on a Cell Vertex Scheme for the Solution of Radiative Transfer Problems in Complex 3D Geometries. *Journal of Quantitative Spectroscopy and Radiative Transfer*, 2011, no. 112, pp. 2661–2675.
11. Modest M.F. *Radiative Heat Transfer*, London, New York, Academic Press Books, 2013.
12. Knaus H., Schneider R., Han X., Strohle J., Schnell U., Hein K.R. Comparison of Different Radiative Heat Transfer Models and Their Applicability in Coal-fired Utility Boiler Simulations. *Proceedings of 4th International Conference on Technologies and Combustion for a Clean Environment*, Lisbon, 1997, pp. 1–8.
13. Howell J.R., Menguc M.P., Siegel R. *Thermal Radiation Heat Transfer*, New York, CRC Press, 2015.
14. Doyoung B., Changjin L., Seung W.B. Radiative Heat Transfer in Discretely Heated Irregular Geometry with an Absorbing, Emitting, and Anisotropically Scattering Medium Using Combined Monte-Carlo and Finite Volume Method. *International Journal of Heat and Mass Transfer*, 2004, no. 47, pp. 4195–4203.
15. Dombrovsky L.A., Dembele S., Wen J.X., Sikic I. Two-Step Method for Radiative Transfer Calculations in a Developing Pool Fire at the Initial Stage of its Suppression by a Water Spray. *International Journal of Heat and Mass Transfer*, 2018, no. 127, pp. 717–726.
16. Gordon I.E., Rothman L.S., Hill C., Kochanov R.V. et al. The HITRAN2016 Molecular Spectroscopic Database. *Journal of Quantitative Spectroscopy and Radiative Transfer*, 2017, no. 203, pp. 3–69.
17. Yujia Sun, Xiaobing Zhang. Contributions of Gray Gases in SLW for Non-Gray Radiation Heat Transfer and Corresponding Accuracies of FVM and P_1 Method. *International Journal of Heat and Mass Transfer*, 2018, no. 121, pp. 819–831. DOI: 10.1016/j.ijheatmasstransfer.2018.01.045
18. Dombrovsky L.A. Evaluation of the Error of the P_1 Approximation in Calculations of Thermal Radiation Transfer in Optically Inhomogeneous Media. *High Temperature*, 1997, vol. 35, no. 4, pp. 676–679.
19. Viskanta R. *Radiative Transfer in Combustion Systems: Fundamentals and Applications*, New York, Begell House, 2005.
20. Litvintsev K.Yu., Dekterev A.A., Neobyavlyashy P.A. Modeling of Radiative Heat Transfer in a Burner Device for Anode Gases Reburning. *Thermal Processes in Engineering*, 2013, vol. 5, no. 8, pp. 354–360. (in Russian)
21. Smith T.F., Shenand Z.F., Friedman J.N. Evaluation of Coefficients for the Weighted Sum of Gray Gases Model. *Journal of Heat Transfer*, 1982, no. 104, pp. 602–608.
22. Yu M.J., Baek S.W., Park J.H. An Extension of the Weighted Sum of Gray Gases Non-Gray Gas Radiation Model to a Two Phase Mixture of Non-Gray Gas with Particles. *International Journal of Heat and Mass Transfer*, 2000, no. 43, pp. 1699–1713.
23. Litvintsev K.Yu., Finnikov K.A., Kharlamov E.B. Features of a Mathematical Model of Heat Transfer in a Vacuum Resistance Furnace. *Journal of Physics: Conference Series*, 2017, no. 891, article ID: 012108. DOI: 10.1088/1742-6596/891/1/012108

24. Litvintsev K.Yu., Finnikov K.A. Development of a Specialized Mathematical Model of Heat Transfer in a Vacuum Electric Furnace. *Journal of Physics: Conference Series*, 2018, no. 1128, article ID: 12088. DOI: 10.1088/1742-6596/1128/1/012088

25. Guedri K., Naceur B.M., Rachid M., Rachid S. Formulation and Testing of the FTn Finite Volume Method for Radiation in 3-D Complex Inhomogeneous Participating Media. *Journal of Quantitative Spectroscopy and Radiative Transfer*, 2006, no. 98, pp. 425–445.

26. Guedri K., AL-Ghamdi A. Radiative Heat Transfer in Complex Enclosures Using NVD Differencing Schemes of the FTn Finite Volume Method. *Heat Transfer Research*, 2017, vol. 48, no. 15, pp. 1379–1398.

27. Kim S.H., Huh K.Y. A New Angular Discretization Scheme of the Finite Volume Method for 3-D Radiative Heat Transfer in Absorbing, Emitting and Anisotropically Scattering Media. *International Journal of Heat and Mass Transfer*, 2000, no. 43, pp. 1233–1242.

28. Barrett R., Berry M.W., Chan T.F., Demmel J.W. *Templates for the Solution of Linear Systems: Building Blocks for Iterative Methods*, Philadelphia, SIAM, 1994.

29. VanderVorst H.A. Bi-CGSTAB: a Fast and Smoothly Converging Variant of Bi-CG for Solution of Non-Symmetric Linear Systems. *SIAM Journal on Scientific Computing*, 1992, no. 2, pp. 631–644.

30. Charest M.R.J., Groth C.P.T., Gulder O.L. Solution of the Equation of Radiative Transfer Using a Newton–Krylov Approach and Adaptive Mesh Refinement. *Journal of Computational Physics*, 2012, no. 231, pp. 3023–3040.

Received March 3, 2021

УДК 536.3+519.6 **DOI: 10.14529/mmp210306**

ПРИМЕНЕНИЕ МЕТОДА КОНЕЧНЫХ ОБЪЕМОВ ДЛЯ РАСЧЕТА ПЕРЕНОСА ИЗЛУЧЕНИЯ В ПРИКЛАДНЫХ ЗАДАЧАХ

К.Ю. Литвинцев[1]***, А.В. Сентябов***[1]
[1]Красноярский филиал, Институт теплофизики им. С.С. Кутателадзе СО РАН, г. Красноярск, Российская Федерация

При разработке в Красноярском филиале ИТ СО РАН комплекса программ «SigmaFlow», предназначенного для решения задач вычислительной гидродинамики и теплообмена, были реализованы математические модели переноса излучения, основанных на использовании P_1 приближения и метода конечных объемов. Реализованный метод конечных объемов позволяет выполнять многопоточные вычисления на основе пространственной декомпозиции расчетной области на неструктурированных сетках. При решении системы линейных алгебраических уравнений для переноса излучения были рассмотрены как стандартные методы, используемые при решении уравнений гидродинамики (BiCGSTAB, DILU, CG), так и схема «бегущего счета». В статье представлены результаты проведенного численного моделирование на базе программы «SigmaFlow» газовой топочной камеры, горелочного устройства и вакуумной электропечи сопротивления, в которых одним из основных механизмов переноса тепла являлось излучение.

Ключевые слова: численное моделирование; вычислительная гидродинамика; программный комплекс.

Кирилл Юрьевич Литвинцев, кандидат физико-математических наук, Красноярский филиал, Институт теплофизики им. С.С. Кутателадзе СО РАН (г. Красноярск, Российская Федерация), sttupick@yandex.ru.

Андрей Васильевич Сентябов, кандидат физико-математических наук, Красноярский филиал, Институт теплофизики им. С.С. Кутателадзе СО РАН (г. Красноярск, Российская Федерация), sentyabov_a_v@mail.ru.

Поступила в редакцию 3 марта 2021 г.